Journal of Physics G: Nuclear and Particle Physics

MAJOR REPORT • OPEN ACCESS

New physics searches with heavy-ion collisions at the CERN Large Hadron Collider

To cite this article: Roderik Bruce *et al* 2020 *J. Phys. G: Nucl. Part. Phys.* **47** 060501

View the article online for updates and enhancements.

Recent citations

- Dark photons from pions produced in ultraperipheral PbPb collisions
  V.P. Gonçalves and B.D. Moreira

- Searching for long-lived particles beyond the Standard Model at the Large Hadron Collider
  Juliette Alimena *et al*
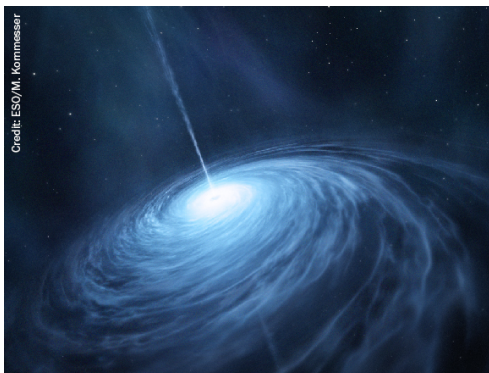
New physics searches with heavy-ion collisions at the CERN Large Hadron Collider

Roderik Bruce[1], David d'Enterria[2,18], Albert de Roeck[2],
Marco Drewes[3], Glennys R Farrar[4], Andrea Giammanco[3],
Oliver Gould[5], Jan Hajer[3], Lucian Harland-Lang[6], Jan Heisig[3],
John M Jowett[1], Sonia Kabana[7,16], Georgios K Krintiras[3,17],
Michael Korsmeier[8,9,10], Michele Lucente[3],
Guilherme Milhano[11,12], Swagata Mukherjee[13],
Jeremi Niedziela[2], Vitalii A Okorokov[14],
Arttu Rajantie[15] and Michaela Schaumann[1]

[1] CERN, BE Department, CH-1211 Geneva, Switzerland
[2] CERN, EP Department, CH-1211 Geneva, Switzerland
[3] Centre for Cosmology, Particle Physics and Phenomenology, Université catholique de Louvain, B-1348 Louvain-la-Neuve, Belgium
[4] Centre for Cosmology and Particle Physics, New York University, NY, NY 10003, United States of America
[5] Helsinki Institute of Physics, University of Helsinki, FI-00014, Finland
[6] Rudolf Peierls Centre, Beecroft Building, Parks Road, Oxford, OX1 3PU, United Kingdom
[7] Department of Physics, University of Nantes, and SUBATECH, 4 rue Alfred Kastler, 44307 Nantes, France
[8] Institute for Theoretical Particle Physics and Cosmology, RWTH Aachen University, Aachen, Germany
[9] Dipartimento di Fisica, Università di Torino, Torino, Italy
[10] Istituto Nazionale di Fisica Nucleare, Sezione di Torino, Torino, Italy
[11] LIP, Av. Prof. Gama Pinto, 2, P-1649-003 Lisboa, Portugal
[12] Instituto Superior Técnico, Universidade de Lisboa, Av. Rovisco Pais 1, 1049-001, Lisboa, Portugal
[13] III. Physikalisches Institut A, RWTH Aachen University, Aachen, Germany
[14] National Research Nuclear University MEPhI, Moscow, Russia
[15] Department of Physics, Imperial College London, London SW7 2AZ, United Kingdom

E-mail: david.d'enterria@cern.ch

[16] Current address: Instituto de Alta Investigación, Universidad de Tarapacá, Casilla 7D, Arica, Chile.
[17] Current address: University of Kansas - Department of Physics and Astronomy Malott Hall, 1251 Wescoe Hall Drive, Lawrence, KS 66045-7582, United States of America.
[18] Author to whom any correspondence should be addressed.

Abstract

This document summarises proposed searches for new physics accessible in the heavy-ion mode at the CERN Large Hadron Collider (LHC), both through hadronic and ultraperipheral $\gamma\gamma$ interactions, and that have a competitive or, even, unique discovery potential compared to standard proton–proton collision studies. Illustrative examples include searches for new particles—such as axion-like pseudoscalars, radions, magnetic monopoles, new long-lived particles, dark photons, and sexaquarks as dark matter candidates—as well as new interactions, such as nonlinear or non-commutative QED extensions. We argue that such interesting possibilities constitute a well-justified scientific motivation, complementing standard quark-gluon-plasma physics studies, to continue running with ions at the LHC after the Run-4, i.e. beyond 2030, including light and intermediate-mass ion species, accumulating nucleon–nucleon integrated luminosities in the accessible fb^{-1} range per month.

Keywords: beyond standard model, heavy ions, LHC

(Some figures may appear in colour only in the online journal)

1. Introduction

Physics beyond the standard model (SM) is necessary in order to explain numerous unsolved empirical and theoretical problems in high energy physics (see e.g. [1] for a recent review). Prominent examples among them are the nature of dark matter (DM), the origin of matter-antimatter asymmetry (baryogenesis), and finite neutrino masses, one the one hand, as well as the Higgs mass fine-tuning, the null θ_{QCD} charge-parity (CP) violation term in quantum chromodynamics (QCD), the origin of fermion families and mixings, charge quantisation, the cosmological constant, and a consistent description of quantum gravity, on the other hand. Most solutions to these problems require new particles—such as supersymmetric partners, dark photons, right-handed neutrinos, axions, monopoles—and/or new interactions, which have so far evaded observation due to their large masses and/or their small couplings to SM particles. Two common complementary routes are followed at colliders in order to search for beyond standard model (BSM) physics. If BSM appears at high masses, one needs to maximise the centre-of-mass (c.m.) energy $\sqrt{s}$. If BSM involves small couplings, one needs to maximise the luminosity $\mathcal{L}$. At face value, both strategies present obvious drawbacks for searches in heavy-ion (HI) compared to pp collisions at the Large Hadron Collider (LHC): (i) PbPb collisions run at roughly 2.5 times lower nucleon–nucleon (NN) c.m. energies than pp collisions ($\sqrt{s_{\text{NN}}} = 5.5$ versus 14 TeV), and (ii) the NN luminosities are about a factor 100 smaller (in 2018, $\mathcal{L}_{\text{NN}} = A^2 \times 6 \times 10^{27} \text{ cm}^{-2} \text{ s}^{-1} = 2.5 \times 10^{32} \text{ cm}^{-2} \text{ s}^{-1}$ for PbPb versus $\mathcal{L}_{pp} = 2 \times 10^{34} \text{ cm}^{-2} \text{ s}^{-1}$).

During the high-luminosity (HL)-LHC phase [2, 3], whose main focus is BSM searches, the luminosity of pp collisions will be maximised, inevitably leading to a large number of overlapping collisions per bunch crossing (pileup). Pileup translates into a rising difficulty to record all interesting pp events, and thereby an unavoidable increase of the kinematical thresholds for triggers and reconstruction objects in order to reduce unwanted backgrounds. Pileup also leads to an intrinsic complication in the reconstruction of exclusive final-states

Table 1. Examples of new-physics particles and interactions accessible in searches with HI collisions at the LHC, listed by production mechanism. Indicative competitive mass ranges and/or the associated measurement advantages compared to the *pp* running mode are given.

Production mode	BSM particle/interaction	Remarks
Ultraperipheral	Axion-like particles	$\gamma\gamma \to a$, $m_a \approx 0.5$–100 GeV
	Radion	$\gamma\gamma \to \phi$, $m_\phi \approx 0.5$–100 GeV
	Born–Infeld QED	Via $\gamma\gamma \to \gamma\gamma$ anomalies
	Non-commutative interactions	Via $\gamma\gamma \to \gamma\gamma$ anomalies
Schwinger process	Magnetic monopole	Only viable in HI collisions
Hard scattering	Dark photon	$m_{A'} \lesssim 1$ GeV, advanced particle ID
	Long-lived particles (heavy ν)	$m_{\text{LLP}} \lesssim 10$ GeV, improved vertexing
Thermal QCD	Sexaquarks	DM candidate

(in particular neutral ones, such as $X \to \gamma\gamma$ decays at not too high masses) and of displaced vertices from e.g. long-lived-particles (LLPs) that appear in many BSM scenarios. In this context, if BSM has low couplings with the SM and is 'hiding well' at relatively low masses with moderately 'soft' final states, HI collisions—with negligible pileup, optimal primary vertexing (thanks to the large number of primary tracks), reduced trigger thresholds (down to zero p_T, in some cases), plus unique and 'clean' $\gamma\gamma$ exclusive final-states in ultraperipheral interactions [4] with luminosities enhanced by factors of order $\mathcal{L}_{\text{PbPb}}(\gamma\gamma)/\mathcal{L}_{pp}(\gamma\gamma) = Z^4 \times \mathcal{L}_{\text{PbPb}}/\mathcal{L}_{pp} = 4.5 \times 10^7 \times (6 \times 10^{27})/(2 \times 10^{34}) \approx 10$—present clear advantages compared to *pp*.

The purpose of this document is to summarise various novel BSM search possibilities accessible at the LHC in the HI mode, and thereby provide new arguments that strengthen the motivations to prolong the HI programme beyond the LHC Run-4 (i.e. after 2029). A selection of new physics (NP) searches that are competitive with (or, at least, complementary to) *pp* studies at the LHC are listed in table 1, and succinctly presented hereafter. This list is not comprehensive, but is representative of the type of processes that are attractive and accessible with ions from the perspective of BSM searches. After a summary of the LHC HI performance of current and future runs (section 2), the document is organised along the following four BSM production mechanisms:

(1) Ultraperipheral $\gamma\gamma$ collisions (UPCs), producing, e.g. axion-like particles (ALPs), section 3.
(2) 'Schwinger' production through strong classical EM fields, producing, e.g. monopoles, section 4.
(3) Hard scattering processes, producing, e.g. displaced signals from new LLPs, section 5.
(4) Thermal production in the quark-gluon-plasma (QGP), producing, e.g. sexaquarks, section 6.

Processes (1), (2), and (4) explicitly use a BSM production mechanism that is unique in HI collisions (or significantly enhanced compared to the *pp* mode), whereas in processes of the

type (3), it is the comparatively reduced pileup backgrounds that renders HI collisions interesting. In addition, detailed studies in proton-nucleus and light-ion collisions are needed as a baseline for astrophysics BSM searches, as well as to explain several anomalies observed in ultra-high-energy cosmic ray (UHECR) data (section 7).

2. Accelerator considerations

The nominal LHC operation schedule includes HI collisions during typically one month each year, and even when accounting for the roughly $\times 10$ lower integrated running time than *pp*, several BSM searches appear more competitive with ions than with protons as shown below. The performance of the HI runs up until the end of Run-2 has been very good, reaching instantaneous PbPb luminosities six times higher than the design value of $10^{27}\,\mathrm{cm^{-2}\,s^{-1}}$ (equivalent to a NN luminosity of $\mathcal{L}_{\mathrm{NN}} = 2.5 \times 10^{32}\,\mathrm{cm^{-2}\,s^{-1}}$). Four LHC experiments are now taking data with HI collisions, and physics runs have also been carried out with a novel mode of operation with *p*Pb collisions that was not initially foreseen [5, 6]. The excellent performance was made possible through many improvements in the LHC and the injector chain. In particular, the average colliding bunch intensity in 2018 was up to about 2.3×10^8 Pb/bunch, which is more than three times higher than the LHC design value. For the next PbPb run in 2021, it is planned to further increase the total LHC intensity through a decrease of the smallest bunch spacing to 50 ns, in order to fit 1232 bunches in the LHC. A further increase of the injected intensity seems difficult without additional hardware in the injector chain [7]. In the LHC, any increase of ion luminosity is ultimately limited by the risk of quenching magnets, either by secondary beams with the wrong magnetic rigidity created in the collisions [8–12] or by leakage from the halo cleaning by the collimators [13–15]. Mitigation of the secondary beam losses around ATLAS and CMS, using an orbit-bump technique, has been demonstrated [16] and additional collimators will be installed in the current long shutdown of the LHC (2019–2020) to allow higher luminosity at IP2 [17] and also to raise the total beam intensity limit from collimation losses [18, 19]. Using the predicted beam and machine configuration, the future luminosity performance has been estimated for PbPb and *p*Pb [20]. During a one-month run, assuming that the instantaneous luminosity is levelled at the current values around $6 \times 10^{27}\,\mathrm{cm^{-2}\,s^{-1}}$, the integrated luminosity per experiment is estimated to be 3.1 nb^{-1} for PbPb and 700 nb^{-1} for *p*Pb (without levelling), equivalent to NN luminosities of $\mathcal{L}_{\mathrm{NN}} \approx 0.15$ fb^{-1}.

In the presently approved CERN planning, it is foreseen to perform another four and a half PbPb runs before the end of LHC Run-4 in 2029, accumulating ~ 13 nb^{-1} in total. Furthermore, one short *p*Pb run is planned, as well as one reference *pp* run. No further HI runs have so far been planned after Run-4. These plans would not permit the full exploitation of the BSM possibilities opened up in HI collisions, which require the largest possible integrated luminosities. A revised proposal for Runs-3 and 4 and plans to extend the LHC nuclear programme beyond Run-4 have been formulated [20]. The additional BSM physics possibilities summarised here complement and reinforce that scientific case. These studies involve more time spent on *p*Pb runs and also collisions of lighter nuclei, e.g. Ar, O, or Kr [20, 21]. Table 2 shows estimated beam parameters and luminosity performance for Pb as well as these lighter species. It can be seen that the latter have the potential to reach $\times(2$–$15)$ higher NN luminosities, which would benefit any BSM search based on hard-scattering processes (section 5), although the corresponding $\gamma\gamma$ luminosities (section 3) would be (naively) reduced by a $(Z_{\mathrm{PbPb}}/Z_{\mathrm{AA}})^4$ factor. The estimated parameters for a range of lighter ions rely on the assumption that the achievable

Table 2. LHC beam parameters and performance for collisions from O up to Pb ions, with a moderately optimistic value of the scaling parameter $p = 1.5$ introduced in [20, 21]. Here σ_{had} is the hadronic cross section, ϵ_n the normalised emittance, and the Z^4 factor is provided to indicate the order-of-magnitude enhancement in $\gamma\gamma$ cross sections expected in UPCs compared to *pp* collisions. Nucleus–nucleus (AA) and NN luminosities $\mathcal{L}$ are given at the start of a fill (to simplify the comparison, it is assumed there is no levelling), $\widehat{\mathcal{L}}$, and as time averages, $\langle\mathcal{L}\rangle$, with typical assumptions used to project future LHC performance. Total integrated luminosities in typical one-month LHC runs are given in the last two rows.
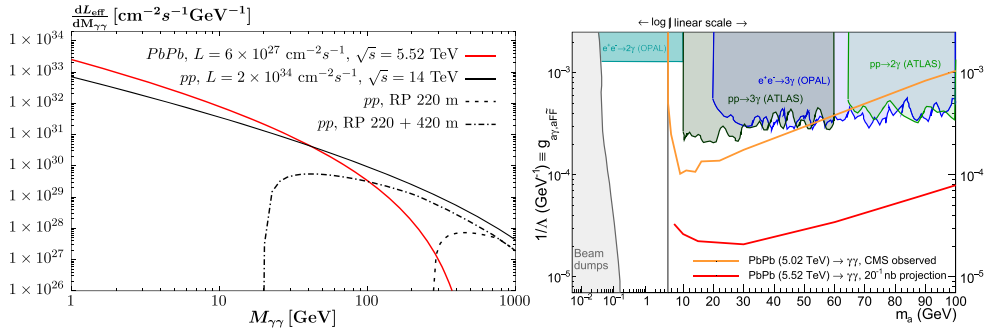
		$^{16}_{8}\text{O}$	$^{40}_{18}\text{Ar}$	$^{40}_{20}\text{Ca}$	$^{78}_{36}\text{Kr}$	$^{129}_{54}\text{Xe}$	$^{208}_{82}\text{Pb}$
γ	(10^3)	3.76	3.39	3.76	3.47	3.15	2.96
$\sqrt{s_{\text{NN}}}$	(TeV)	7	6.3	7	6.46	5.86	5.52
σ_{had}	(b)	1.41	2.6	2.6	4.06	5.67	7.8
N_b	(10^9)	6.24	1.85	1.58	0.653	0.356	0.19
ϵ_n	(μm)	2	1.8	2	1.85	1.67	1.58
Z^4	(10^6)	4.1×10^{-3}	0.01	0.16	1.7	8.5	45
$\widehat{\mathcal{L}}_{\text{AA}}$	$(10^{30}\ \text{cm}^{-2}\,\text{s}^{-1})$	14.6	1.29	0.938	0.161	0.0476	0.0136
$\widehat{\mathcal{L}}_{\text{NN}}$	$(10^{33}\ \text{cm}^{-2}\,\text{s}^{-1})$	3.75	2.06	1.5	0.979	0.793	0.588
$\langle\mathcal{L}_{\text{AA}}\rangle$	$(10^{27}\ \text{cm}^{-2}\,\text{s}^{-1})$	8990	834	617	94.6	22.3	3.8
$\langle\mathcal{L}_{\text{NN}}\rangle$	$(10^{33}\ \text{cm}^{-2}\,\text{s}^{-1})$	2.3	1.33	0.987	0.576	0.371	0.164
$\int_{\text{month}} \mathcal{L}_{\text{AA}}\text{d}t$	(nb^{-1})	1.17×10^4	1080	799	123	28.9	4.92
$\int_{\text{month}} \mathcal{L}_{\text{NN}}\text{d}t$	(fb^{-1})	2.98	1.73	1.28	0.746	0.480	0.210

bunch intensity N_b for a nucleus with charge number Z and mass number A can be scaled from the Pb bunch intensity as $N_b(Z, A) = N_b(82, 208) \times (Z/82)^p$, where the power $p = 1.5$ is estimated from previous experience of nuclear beams for the CERN fixed-target experiments and the short run with Xe in the LHC in 2017 [22]. It should be noted that these estimates carry a significant uncertainty, since there have been no opportunities to experimentally optimise these beams for the LHC. Furthermore, the integrated luminosity per month in table 2 has been calculated using a simplified model, and no levelling of luminosity, which gives slightly more optimistic values for Pb than the 3.1 nb^{-1} stated above, that was simulated with a more detailed and accurate model. Total integrated luminosities in the range 0.2–3 fb^{-1} are expected depending on the ion–ion colliding system. We stress that, if BSM or other physics cases eventually justify it, one can consider running a full '*pp* year' with ions at the LHC, leading to roughly factors of $\times 10$ larger integrated luminosities than those listed in table 2.

3. Ultraperipheral $\gamma\gamma$ collisions

In HI collisions, the highly relativistic ions act as a strong source of electromagnetic (EM) radiation, enhanced by the large proton charge number Z [4]. This offers a natural environment in which to observe the photon-initiated production of BSM states with QED couplings. The cross section for the $\gamma\gamma$ production of any particle X can be calculated within the equivalent photon approximation [23] as

$$\sigma_{A_1 A_2 \to A_1 X A_2} = \int \text{d}x_1 \text{d}x_2\, n(x_1) n(x_2) \widehat{\sigma}_{\gamma\gamma \to X} = \int \text{d}m_{\gamma\gamma} \frac{\text{d}\mathcal{L}_{\text{eff}}}{\text{d}m_{\gamma\gamma}} \widehat{\sigma}_{\gamma\gamma \to X}, \tag{1}$$

Figure 1. Left: effective $\gamma\gamma$ luminosity versus photon-fusion mass in ultraperipheral PbPb and *pp* collisions at the LHC. In the *pp* case, the actually 'usable' $\gamma\gamma$ luminosity is also shown with proton tagging at 220 m (currently installed) and 420 m (proposed). Right: exclusion limits (95% confidence level) in the ALP-γ coupling ($g_{a\gamma}$) versus ALP mass (m_a) plane [25, 26] currently set in *pp* and e^+e^- (shaded areas) compared to those from PbPb UPC measurements (CMS result today [25, 26], orange curve; and projections for 20 nb^{-1}, bottom red curve).

where x_i is the longitudinal momentum fraction of the photon emitted by ion A_i. This factorises the result in terms of a $\hat{\sigma}(\gamma\gamma \to X)$ subprocess cross section of a (BSM) system X, and fluxes $n(x_i)$ of photons emitted by the ions. The latter are precisely determined in terms of the ion EM form factors, and are in particular enhanced by $\propto Z^2$ for each ion, leading to an overall $\sim Z^4$ enhanced production in ion–ion compared to *pp* collisions (i.e. a factor of $\sim 5 \times 10^7$ for PbPb). The experimental signal of UPC processes is very clean with the system X and nothing else produced in the central detector. Moreover, since the virtuality of the emitted photons is restricted to be very small $Q^2 \sim 1/R_A^2$, where R_A is the ion radius, the X object is produced almost at rest [4]. The impact parameters $b_\perp$ of UPCs with ions, with $b_\perp \gg 2R_A$ beyond the range of additional strong interactions, are significantly larger than in the *pp* case, and the associated gap survival probability is also significantly bigger than for EM proton interactions. This latter effect can be accounted for precisely and enters at the $\mathcal{O}(10\%)$ level in terms of corrections to $\gamma\gamma$ interactions, with rather small uncertainties [24]. In addition, the background from QCD-initiated production is essentially completely removed by the requirement that the system X and nothing else is seen in the central detector [24].

A wide programme of photon-photon measurements and theoretical work is ongoing in the context of *pp* collisions at the LHC [27], with dedicated proton taggers (Roman Pots, RP) installed inside the LHC tunnel at $\sim$220 m from the ATLAS [28] and CMS [29] interaction points. In comparison to the *pp* mode, UPCs with HI offer the distinct advantage of studying such photon-fusion processes in an environment where pileup is absent, forward tagging is unnecessary, and considerably lower masses can be probed. Indeed, two-photon processes in *pp* collisions at high luminosity can only be observed by tagging the forward protons inside the LHC tunnel with geometrical acceptances that bound any central system to have, at least, $m_X \gtrsim 100$ GeV. Figure 1 (left) compares the effective $\gamma\gamma$ luminosity as a function of $m_{\gamma\gamma}$, defined in cross section (1), for *pp* and PbPb collisions at their nominal c.m. energies and instantaneous luminosities. Even after accounting for the reduced beam luminosity in PbPb collisions, the effective $\gamma\gamma$ luminosity is a factor of two higher in PbPb than the (purely theoretical) *pp* values at low masses. As a matter of fact, taking into account the acceptance in the proton fractional momentum loss ξ of the RP detectors at 220 m ($0.02 < \xi < 0.15$) [28, 29] and even including proposed RPs at 420 m ($0.0015 < \xi < 0.15$) [30], only PbPb enables studies in the region below $m_X \approx 100$ GeV.

Running *pp* at low pileup would cover the low mass region albeit with significantly reduced $\gamma\gamma$ luminosities. Various relevant $\gamma\gamma$ BSM processes are available in the SUPERCHIC [24] and STARLIGHT [31] Monte Carlo (MC) generators, and ion fluxes are also available for any process generated with MADGRAPH [32].

3.1. Axion-like particles

ALPs constitute a class of pseudoscalars with couplings to SM fermions or gauge bosons through dimension-5 operators. In some cases, they may be Goldstone bosons of an approximate, spontaneously broken, global symmetry. In this sense they are inspired by original axions arising from the Peccei–Quinn mechanism to solve the absence of CP violation in QCD [33, 34], but in general they do not have to solve the strong CP problem, and are therefore to be understood as purely phenomenological extensions of the SM. An ALP couples to photons through the operator $\mathscr{L} \supset \frac{a}{4f}F_{\mu\nu}\widetilde{F}^{\mu\nu}$, where f is the decay constant of the ALP. They can be produced through photon-fusion $\gamma\gamma \to a$ or associated $f\bar{f} \to \gamma a$ production, where the latter tends to be the strongest production mode at electron or proton machines. In the mass range below about 100 GeV, photon fusion in ultraperipheral HI collisions is competitive thanks to the huge Z^4 enhancement in the photon luminosity [25] (figure 1, right).

A second key feature is that the only SM background is light-by-light (LbL) scattering, which is notoriously tiny [35]. This means that it is crucial that the Lagrangian $\mathscr{L}$ above provides the dominant coupling of the ALP to the SM: any competing branching ratios to leptons or jets would degrade the reach, as the backgrounds in those final states are unsuppressed. Evidence and/or observation for LbL scattering in PbPb UPCs has been reported by ATLAS [36, 37] and CMS [26]. The latter one also provides the best current limits on ALPs in the mass range from $m_a = 5$ to 50 GeV for coupling to photons only (figure 1 right), and $m_a = 5$ to 10 GeV for a scenario with hypercharge coupling as well. For a recast of the ATLAS data to a limit on ALPs, see [20, 38]. Given that the higher mass ALPs will be well covered by the regular *pp* runs, PbPb collisions will likely remain the only choice when searching for ALPs up to $m_a \approx 100$ GeV, though a comparison of the higher-mass reach for lighter ions would be interesting. Going below $m_a < 5$ GeV is not possible for ATLAS and CMS, due to trigger and noise limitations in the calorimeters, but the range $m_a \approx 0.5$–5 GeV can be covered by UPC measurements in ALICE and LHCb, complementing a mass range that Belle II is also expected to measure reasonably well [39]. Finally, as more data are gathered, the LbL background will become a limitation. The limits would therefore benefit substantially if the diphoton invariant mass resolution could be improved, possibly by making use of γ conversions.

3.2. Born–Infeld nonlinear QED, non-commutative QED

The possibility of nonlinear Born–Infeld (BI) extensions of QED has a long history, first proposed in the 1930s [40], they appear naturally in string-theory models [41]. Remarkably, however, the limit on the mass scale of such extensions has until recently been at most at the level of 100 MeV [42]. The first LHC measurement of LbL scattering in HI collisions [36] has enabled to extend the upper limit of nonlinear QED modifications by 3 orders of magnitude, up to scales $\Lambda_{\mathrm{BI}} \gtrsim 100$ GeV, which in turn imposes a lower limit of 11 TeV on the magnetic monopole mass in the case of a BI extension of the SM in which the $U(1)_Y$ hypercharge gauge symmetry is realised nonlinearly [42]. Future LbL measurements in HI UPCs will offer the possibility to further probe Born–Infeld and other nonlinear extensions of QED.

Non-commutative (NC) geometries also naturally appear within the context of string/M-theory [43]. One consequence of this possibility is that QED takes on a non-Abelian nature

due to the introduction of three- and four-point functions, leading to observable signatures in the total and differential cross sections of QED processes. In [44] it has been demonstrated that NC effects impact $\gamma\gamma \to \gamma\gamma$ scattering at tree-level, and that a study of its differential cross sections at a photon-collider in the few hundred of GeV range can bound NC scales of order a TeV. Somewhat lower limits (in the few hundred GeV range for the NP scale) can be reached through the detailed study of the LbL process accessible in UPCs with ions at the LHC.

3.3. Other BSM particles

There are several other possible BSM signals that couple to a pair of photons. It has been argued e.g. that $\gamma\gamma \to \gamma\gamma$ collisions can be used to search for radions [45], gravitons [46, 47] and unparticles [48]. The UPC signatures would be resonances and/or a non-trivial interference pattern of these new contributions with the SM LbL background. The scalar radion would behave identically to the pseudoscalar ALP example discussed in section 3.1. Evaluating the search potential requires dedicated studies, in particular to compare with the reach of other studies sensitive to these models, such as the mono-photon searches in standard *pp* collisions. In the case of unparticles, unitarity and bootstrap bounds must be accounted for as well [49–51].

Charged supersymmetric (SUSY) particles like sleptons and charginos are also natural targets for $\gamma\gamma$ collisions, especially in the squeezed regime where the standard lepton-plus-missing-E_T searches lose sensitivity. Although the parameter space accessible to HI collisions has already been ruled out by LEP for simplified SUSY scenarios, it may be possible to extract a competitive limit with $\gamma\gamma$ collisions from the proton beams [52, 53].

Magnetic monopoles necessarily couple strongly to photons [54]. Hence it has been suggested that $\gamma\gamma$ collisions are a natural candidate for monopole searches, either by direct detection [55–58], by the formation of monopolium bound-states [56, 57, 59] or via the contribution of virtual monopole loops to LbL scattering [60–62]. However, these approaches have been criticised for their reliance on perturbative loop expansions in the strong monopole coupling [63, 64]. Such limitations are circumvented in the production mechanism from classical EM fields discussed next.

4. Strong EM fields

4.1. Magnetic monopoles

There are compelling theoretical reasons for the existence of magnetic monopoles [54, 65, 66], such as providing a mechanism to explain charge quantisation in the SM. Consequently, there have been many searches [67], including currently a dedicated LHC experiment, MoEDAL [68]. Due to the Dirac quantisation condition, magnetic monopoles are necessarily strongly coupled, hence perturbative loop expansions for their cross sections cannot be trusted. In fact, it has been argued that the pair production cross section of semi-classical monopoles [69, 70] in *pp* or elementary particle collisions suffers from an enormous non-perturbative suppression [71–73], $\sigma_{M\overline{M}} \propto e^{-4/\alpha} = 10^{-238}$, independent of collision energy. It is not known if the same suppression applies to point-like elementary monopoles, but if it does [74], it implies that magnetic monopoles cannot realistically be produced in *pp* collisions, irrespective of the energy and luminosity of the collider. The assumptions that led to the exponential cross section suppression do not apply to HI collisions due to the non-perturbatively large magnetic fields that are produced, which are strongest in UPCs [75]. These fields may produce magnetic monopoles by the EM dual of Schwinger pair production [76], the calculation of which does not rely on perturbative expansions in the coupling. To date, there has only been one search for magnetic monopoles in HI collisions, conducted at
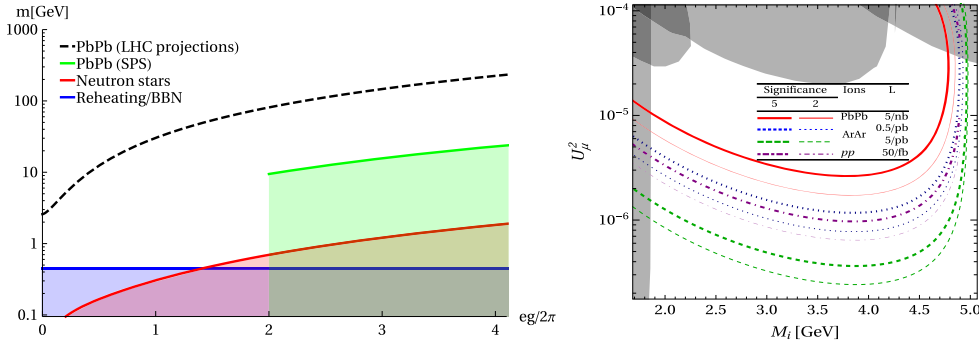
Figure 2. Left: lower bounds for the magnetic monopole mass (m) versus units of magnetic charge ($e \cdot g/2\pi$) [78]. Right: estimated CMS reach for heavy neutrinos, with mass M_i and muon-neutrino mixing angle U_μ, from B-meson decays in pp, ArAr, and PbPb collisions with equal running time [79].

SPS [77], which has led to the strongest bounds on their mass [78]. Searches in HI collisions at the LHC could in principle produce 2–3 orders of magnitude heavier monopoles, directly testing their existence in the hundreds of GeV mass range for the first time (figure 2, left).

From the experimental point of view, triggering and tracking constitute challenges for the LHC experiments. Magnetic monopoles would manifest as highly ionising particles, and their trajectories in a uniform magnetic field are parabolic. These are striking features that, on the one hand, help to reject background events to very small levels and, on the other, may cause monopoles to be missed by standard reconstruction algorithms, as a basic assumption of charged-particle tracking is that particle trajectories are helical. Given that their production by strong magnetic fields is most likely in UPCs, the usual UPC signature of an almost empty detector would be exploitable to select monopole events. Alternatively a monopole search can be carried out using passive trapping detectors, exploiting the absolute stability of monopoles as used in the MoEDAL experiment [68], during the HI running mode. Unlike active detectors, this method gives no direct information about the process that produced the monopole, but it has the advantage that there is no SM background and therefore no risk of a false positive event.

5. Hard scattering processes

5.1. Long-lived particles

Many BSM models predict the existence of LLPs that can travel macroscopic distances after being produced, see e.g. [80, 81]. Their existence is in many cases linked to the solution of fundamental problems in particle physics and cosmology, such as the origin of neutrino masses, the DM puzzle, or baryogenesis. The LLPs usually owe their longevity to a (comparably) light mass, a feeble coupling to ordinary matter, or a combination of both. If such particles are produced in HI collisions, the feeble interaction allows most of them to leave the quark-gluon plasma unharmed. Due to the long lifetime, the tracks from their decay into SM particles can easily be distinguished from the large number of tracks that originate from the collision point (a single one, given the absence of pileup when running in the HI mode). Hence, HI collisions can potentially provide a cleaner environment for LLP searches than pp. The main obstacle is the considerably lower luminosity in HI compared to proton runs, which means that the total number of LLPs produced in the former is always much smaller than in

the latter. However, there are at least three factors that can make the observable number of LLP events competitive [79, 82].

First, due to the absence of pileup, the probability of misidentifying the primary vertex is practically negligible for HI collisions because all tracks originate from a small (fm-sized) region. This is in contrast to the HL-LHC pileup with proton beams, which leads to a comparable number of tracks as a single PbPb collision [2, 3] originating from different points in the same bunch crossing and thereby creating a considerable combinatorial track background for displaced signatures. HI collisions entirely remove the problem of identifying the location of the primary vertex, which may be the key to trespass the 'systematics wall' due to uncertainties in cases where background contamination mostly comes from real (as opposed to misidentified or fake) SM particles. Although a large track multiplicity is expected to degrade the reconstruction and identification of displaced vertices, the adverse effect of pileup on vertex-finding performance is coming more from the presence of additional primary-interaction vertices than from the sheer number of tracks, as demonstrated by the better b-quark tagging performance in pPb compared to pp collisions in $t\bar{t}$ studies [83].

Second, absence of pileup allows the detectors to be operated with minimal (zero bias) triggers. This is an advantage e.g. in scenarios in which LLPs lead to low-p_T final states. Third, in addition to the hard scatterings that we focus on here, HI collisions can offer entirely new production mechanisms that are absent in proton collisions, such as production in the strong EM fields discussed in sections 3 and 4 or in the thermal processes mentioned in section 6.

In [79, 82], it has been shown for the specific example of heavy neutrinos that the zero-bias triggers alone can make searches for typical LLP signatures competitive in HI collisions. Such heavy-ν could simultaneously explain the masses of the SM neutrinos and the baryon asymmetry of the Universe [84]. For masses below 5 GeV, heavy neutrinos are primarily produced in the decay of B-hadrons along with a charged lepton, but the lepton p_T is too small to be recorded by conventional pp triggers, making more than 99% of the events unobservable. As a result, the observable number of events per running time in PbPb with low-p_T triggers is comparable to that in pp collisions with conventional triggers: $5 \, \text{nb}^{-1}$ of lead collisions could improve the current limits by more than one order of magnitude in comparison to current bounds. For a small range of masses over 4 GeV the improvement would even be of two orders of magnitude. If lighter nuclei are used, allowing for higher luminosities (table 2), then HI collisions can yield a larger number of observable LLP events per unit of running time than pp (figure 2, right) [79].

We should emphasise that we refer to the heavy neutrino example here because it is the only case that has been studied in detail so far. It is a very conservative example because it only takes advantage of one of the three factors mentioned above, namely the lower p_T triggers. In models that predict an event topology that suffers from backgrounds due to pileup, or LLPs that can be produced through one of the new mechanisms mentioned above (such as ALPs) HI data will have an even bigger impact.

5.2. Dark photons

The dark photon A' is a hypothetical extra-U(1) gauge boson that acts as a messenger particle between a dark sector, constituted of DM particles, and couples with a residual interaction g to the SM particles. If the dark photon is the lightest state of the dark sector it can only decay into SM particles. Typical experimental searches focus on A' decays to dielectrons (if $m_{A'} < 2m_\mu$), dimuons (for A' masses above twice the muon mass) or dihadrons, and have so far constrained its existence in the mixing parameter g^2 versus mass $m_{A'}$ plane. Collider
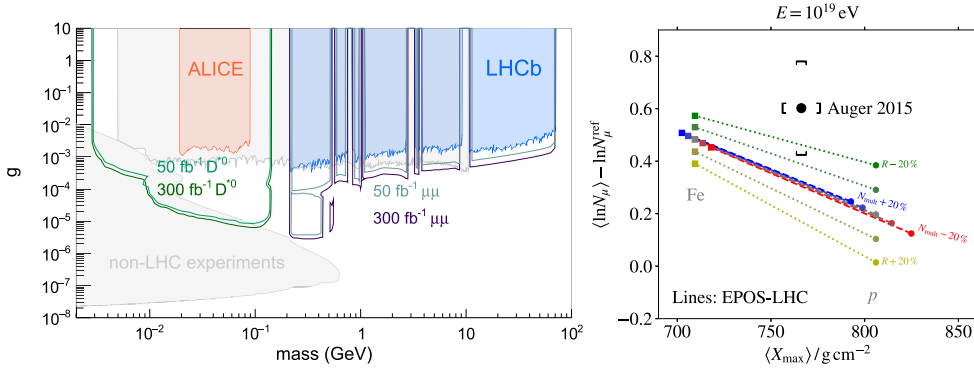
Figure 3. Left: 90% CL exclusion limits of the dark photon mixing parameter *g* as a function of its mass. Red and blue regions show updated projections from measurements at ALICE and LHCb [20]. Light grey bands include results from BABAR, KLOE, A1, APEX, NA48/2, E774, E141, E137, KEK, Orsay, BESIII, CHARM, HPS, NA64, NOMAD, NuCAL, and PS191 [86]. Right: data-MC deviations in the logarithm of the number of muons produced by a 10^{19} eV CR shower versus its maximum depth in the atmosphere (X_{max}): data from Auger [87] are compared to MC predictions for proton and Fe-ions CR primaries with varying values of the default MC hadron multiplicity N_{mult} and the energy fraction α that goes into neutral pions. (Figure taken from [88].)

experiments search for the $A' \to \ell^+ \ell^-$ in Dalitz meson decays π^0, η, $\eta' \to \gamma A'$; meson decays $K \to \pi A'$, $\phi \to \eta A'$, and $D^* \to D^0 A'$; radiative decays of vector-meson resonances Υ (3*S*) in BaBar; and $\phi \to e^+ e^-$ in KLOE in $e^+ e^-$ collisions [20]. HI experiments often feature excellent capabilities for electron and muon identification at low transverse momenta, and for vertexing, leading to competitive searches for low-mass A' from large samples of meson Dalitz decays (see e.g. [85] for PHENIX limits in *pp* and *d*Au collisions at the RHIC collider). As an example of HI feasibility, ALICE is expected to reach a limit in *g* of about 10^{-4} at 90% confidence level (CL) for A' masses 20–90 MeV with *pp*, *p*Pb and PbPb collisions in Run-3 [20] (figure 3, left). Such limits may eventually be superseded by LHCb and fixed-target experiments [86], although any increase in the total HI integrated luminosities, e.g. running with lighter ions as advocated here, can render the former competitive.

6. Thermal processes

6.1. Sexaquarks

The sexaquark *S* is a hypothesised neutral stable dibaryon *uuddss* system that can account for DM in the Universe. The *S* would likely have a mass in the range $m_S \approx 2m_p \pm m_\pi$, and would have escaped detection to date [89]. The quark content of the sexaquark is the same as that of the H-dibaryon proposed by Jaffe in 1977 [90]. However, the H-dibaryon was assumed to be relatively loosely bound with a weak-interaction lifetime; such a particle has been extensively searched for and not found, as discussed in [89]. Being a flavour singlet, the lightest particle to which it could be significantly coupled is the flavour singlet superposition of ω–ϕ, leading to an estimated size of $r_S = 0.1$–0.2 fm [91]. If a stable sexaquark exists, it is an attractive DM candidate because the sexaquark-to-baryon density ratio can be predicted by simple statistical arguments in the QGP-hadronisation transition with known QCD parameters

(quark masses and T_{QCD}) to be $\approx 4.5 \pm 1$, in agreement with the observed DM-to-baryon ratio $\Omega_{\mathrm{DM}}/\Omega_b = 5.3 \pm 0.1$. This ratio is not modified during the subsequent universe expansion as long as $r_S \lesssim 0.2\,\mathrm{fm}$ [91], thereby evading the counter-arguments against dibaryon DM given in [92–94].

If a stable or weakly-decaying dibaryon exists, its production in HI collisions can be completely predicted as a function of its mass, the temperature T, and the local baryon chemical potential μ_b of the produced QGP. A rough estimate for the central rapidity region, assuming $m_S = 2m_p$, $T = 150\,\mathrm{MeV}$, and $\mu_b = 0$, gives $\{\pi{:}n{:}S\} \approx \{1{:}0.01{:}10^{-4}\}$. If the entire rapidity range were to come into thermal equilibrium, so that the excess baryon number B of the initial ions is uniformly distributed in rapidity over the final state, in analogy with early universe conditions, it would imply $N_S - N_{\bar{S}} = \Omega_{\mathrm{DM}}/\Omega_b(m_p/m_S)(N_B - N_{\bar{B}})$. Measuring the dependence of S and $\bar{S}$ production on $\sqrt{s_{\mathrm{NN}}}$, colliding species, and rapidity would be very revealing and could directly connect DM production in HI collisions to that in the early universe.

Demonstrating that S and $\bar{S}$ are produced and measuring their production rates is difficult due to the vastly greater abundance of (anti)deuterons with similar mass to m_S and larger scattering and annihilation cross sections in the detector. Studies are underway to understand the accuracy with which different techniques can identify the production of S and $\bar{S}$, either exploiting the excellent hadron-identification capability over a wide momentum range in ALICE and LHCb, or the larger acceptance of the multi-purpose ATLAS and CMS detectors. Three basic approaches are being considered [89]:

- S particles produced in the primary collision can annihilate with a nucleon in the tracker material and produce a final state with $B = -1$, $S = +2$. LHC detectors can search for $\bar{S}p \rightarrow K^+\bar{\Lambda}^0$ or $\bar{S}n \rightarrow K^0\bar{\Lambda}^0$. The $\bar{\Lambda}^0$ is readily identified; in the absence of an $\bar{S}$, $\bar{\Lambda}^0$ production is only consistent with baryon number conservation if the collision is initiated by an antibaryon and the $\bar{\Lambda}^0$ is accompanied by a baryon. Due to the significant penalty for producing a two-body final state, the rate could be several orders of magnitude greater if the analysis could be extended to events with >2 final particles coming from the vertex.
- Given the $\mathcal{O}(10^{-2})$ production rate of S or $\bar{S}$ relative to single baryons, there may be comparable numbers of events with an $S\bar{S}$ pair or with just a single S or $\bar{S}$ produced, with B and strangeness numbers balanced by two (anti)baryons and 0–2 kaons. It may be possible to establish a systematic correlation of missing $\Delta B = \mp 2$; $\Delta S = \pm 2$ on a statistical basis.
- A population of neutral interacting and/or annihilating particles, distinct from n and $\bar{n}$ by virtue of having different scattering and annihilation cross sections (and different final states, if that is incorporated into the analysis), is in principle discernible by plotting the rate of such reactions as a function of the tracker material grammage and searching for additional exponential components.

6.2. Magnetic monopoles

For central collisions in which a thermal fireball is created, magnetic monopoles may, in principle, be created thermally. Although their microphysical cross sections are not known due to the strong coupling of magnetic monopoles, it seems reasonable to assume that there would exist some production mechanism in a thermal bath containing particles that couple to them (such as photons). Thus, if a temperature T is reached in a given HI collision, one would expect to produce monopoles with masses $m \lesssim T$, and an order of magnitude or so heavier when integrated over the luminosity. Studies based on this production channel would provide

an approach to monopole searches independent from, and complementary to, that of production by strong fields (section 4.1). However, at LHC energies one would expect production by strong fields to dominate as $T^2 \sim 0.3\,\text{GeV}^2 \ll gB \sim 100\,\text{GeV}^2$, where $g = 2\pi/e$ is the minimum magnetic charge [54] and B is the magnetic field produced in a typical UPC [75]. The experimental signatures would be as for section 4.1, except that in this case more central HI collisions are favoured.

6.3. Other NP searches in the QGP

Studies of other novel QCD phenomena benefit from the larger HI integrated luminosities proposed here:

- Various forms of strange-quark matter proposed as DM candidates, such as strange-quark nuggets [95] or magnetised quark nuggets [96], can form with enhanced rates through thermal production and/or coalescence of partons. The production of any new hypothesised stable multiparton states is therefore expected to be only possible or significantly enhanced out of the hadronizing hot and dense QGP formed in HI collisions.
- The absence of CP violation in the QCD sector of the SM is a typical case of theoretical fine-tuning that motivates the existence of new BSM particles, such as the axion [33, 34]. An alternative perspective to this problem is provided by finite-temperature studies of the QCD vacuum, whose non-trivial topology leads to the presence of metastable domains with properties determined by the discrete P/CP symmetries. Decays of such domains, or classical transitions (sphalerons) among them, in the deconfined QGP phase with restored chiral symmetry can result in local violation of P/CP invariance, leading e.g. to the so-called 'chiral magnetic effect' in HI collisions [97].

7. HI input for NP searches with cosmic rays (CRs)

Beyond colliders, searches for NP are currently carried out also via CR measurements. There are at least two concrete areas where HI data are needed in order to improve the SM theoretical baseline and identify possible BSM signals: (i) precision measurements of antiproton and antinuclei production of relevance for DM searches in space experiments at energies $E_{\text{CR}} \approx 10^{13}$–$10^{15}$ eV, and (ii) precision measurements of nuclear effects of relevance for muon production in CR interactions with nuclei in the atmosphere at energies (well) above the LHC range[19] ($E_{\text{CR}} \approx 10^{17}$–$10^{20}$ eV).

7.1. Astrophysical DM searches

Cosmic-ray antiproton and antinuclei have long been considered as potential NP signals, as products e.g. of DM annihilation, and their detection is a major goal of the AMS-02 experiment on-board the international space station [98]. Precise collider measurements of the production cross sections of antiprotons and heavier secondaries in nuclear interactions are crucial ingredients for probing the underlying space propagation [99, 100], and identifying the origin of various excesses observed in the data [101] with respect to model predictions [102–106]. For instance, a recent measurement of antiproton production in pHe collisions with the SMOG device of the LHCb experiment [107] has significantly improved the

---

[19] The LHC pp c.m. energy, $\sqrt{s} = 14$ TeV, corresponds to UHECR of $E_{\text{CR}} \approx 10^{17}$ eV colliding with air nuclei at rest in the upper atmosphere.

antiproton cross-section parametrisation [108] used in the interpretation of AMS-02 data [109]. In the absence of NP, the production of light anti(hyper)nuclei is thought to proceed via thermal hadronisation and nucleon coalescence. The cross section for antinucleus production can be parametrised from the ratio of antiproton cross sections in pA and pp collisions combined with A-dependent coalescence factors B_A, that need to be experimentally obtained [20]. From the ratios of B_A factors in pA and pp, one can predict CR flux ratios for a given antinucleus of atomic number A. The current B_A measurements [110] are confined to mid-rapidity, and have uncertainties larger than the precision required on the CR flux for DM astrophysical searches. Extended LHC running with various ion species is needed to reduce such uncertainties in searches for astrophysical BSM signals via CR antiproton and antinuclei measurements.

7.2. Anomalies in UHECR showers

The collisions in the upper atmosphere of the highest-energy CR ever detected, with $E_{CR} \approx 10^{20}$ eV corresponding to $\sqrt{s_{NN}} \approx 400$ TeV, are well beyond the reach of foreseeable-future colliders [111]. The flux of UHECRs impinging on the Earth is very scarce (less than 1 particle per km^2 per century at the highest energies), and their detection is only possible in dedicated observatories that reconstruct the huge extensive air showers (EAS) of secondary particles that they produce in the atmosphere. Measurements of UHECR above LHC energies, $E_{CR} \approx 10^{17}$–10^{20} eV, feature 30%–60% more muons produced at ground and at increasingly larger transverse momenta from the EAS axis, than predicted by all UHECR MC models [87, 112–114]. Shown in figure 3 (right) is a representative measurement by the Pierre Auger Observatory [87] showing the data-MC deviation in the number of muons from a 10^{19} eV CR shower versus the maximum depth of the shower in the atmosphere. The data point is systematically above the EPOS-LHC MC predictions for varying values of relevant model parameters [88]. Studies based on PYTHIA 6 [115] indicate that additional muon production from hard processes, such as from e.g. jets or heavy-quark decays, do not seem to account for the data-model discrepancy. The possibility of an additional hard source of muons due to the early production and decay of BSM particles, such as e.g. electroweak sphalerons [116], remains an intriguing possibility. Solution of the 'muon puzzle' in UHECR physics requires to reduce the uncertainties on the nuclear effects that remain in the dominant pAir (or FeAir) interactions in the top atmosphere. Dedicated runs of pO [20] and light-ion collisions at the LHC are therefore required in order to improve the modelling and tuning of all nuclear effects in the current hadronic MC simulations, before one can consider any BSM interpretation of UHECR anomalies.

8. Summary

The scientific case for exploiting HI collisions at the LHC in searches for BSM physics has been summarised. A non-comprehensive but representative list of BSM processes accessible with HI at the LHC has been presented based on four underlying mechanisms of production: $\gamma\gamma$ fusion in ultraperipheral collisions, 'Schwinger' production through strong classical EM fields, hard scattering processes, and thermal production in the QGP. Such searches provide additional motivations, beyond the traditional QGP physics case, to prolong the HI programme past their currently scheduled end in 2029 (Run-4), in particular running with lighter ion systems, a LHC operation mode that has not been considered so far. Despite the lower nucleus–nucleus c.m. energies and beam luminosities compared to pp collisions, HI are more

competitive than the latter in particular BSM scenarios, whereas in some others they can complement or confirm searches (or discoveries) performed in the *pp* mode.

Ultraperipheral collisions (UPC) of ions offer, in particular, a unique way to exploit the LHC as an intense $\gamma\gamma$ collider, profiting from the $\sim Z^4$ enhancement factor in their cross sections, providing a clean and well understood environment within which to search for BSM states with QED couplings at masses $m_X \lesssim 100$ GeV that are otherwise not accessible in the *pp* mode. The UPC discovery potential for new particles, such as axion-like pseudoscalar or radions, and/or new interactions, such as nonlinear Born–Infeld or non-commutative QED interactions, is unrivalled in this mass range. For magnetic monopoles, the huge EM fields present in HI collisions lead to exponential enhancements of their cross sections and allow for first-principles calculations that are otherwise hindered in similar *pp* analyses. Central HI collisions provide also a propitious environment for searching for a possible stable sexaquark (QCD DM candidate).

In the case of BSM signals produced through hard scatterings, the absence of pileup, the improved primary and displaced vertexing, and the lower trigger thresholds of HI compared to *pp* collisions, provide superior conditions for searches for BSM LLPs at low masses: an illustrative case has been made based on right-handed neutrinos with $m_\nu \lesssim 5$ GeV, where the higher luminosities attainable with lighter ions lead to a larger number of observable LLP events per unit of running time than in *pp* collisions. The improved particle identification capabilities and lower p_T thresholds of the ALICE and LHCb experiments make them also competitive detectors for dark-photon searches. Both LLPs and dark photon searches would benefit from the increased NN luminosity accessible in collisions with light- and intermediate-ion species. Extrapolations based on the current LHC performance indicate that NN integrated luminosities in the fb^{-1} range per month can be easily achieved with lighter ions after the Run-4.

Acknowledgments

ORCID iDs

David d'Enterria ⓘ https://orcid.org/0000-0002-5754-4303
Marco Drewes ⓘ https://orcid.org/0000-0003-0521-7586
Glennys R Farrar ⓘ https://orcid.org/0000-0003-2417-5975
Andrea Giammanco ⓘ https://orcid.org/0000-0001-9640-8294
Jan Hajer ⓘ https://orcid.org/0000-0001-8083-9102
John M Jowett ⓘ https://orcid.org/0000-0002-9492-3775
Georgios K Krintiras ⓘ https://orcid.org/0000-0002-0380-7577
Michele Lucente ⓘ https://orcid.org/0000-0002-5778-6425
Jeremi Niedziela ⓘ https://orcid.org/0000-0002-9514-0799

Vitalii A Okorokov ⬤ https://orcid.org/0000-0002-7162-5345
Arttu Rajantie ⬤ https://orcid.org/0000-0002-6406-4412
Michaela Schaumann ⬤ https://orcid.org/0000-0002-4943-7698

References

[1] Cid Vidal X *et al* 2019 Report from Working Group 3 *CERN Yellow Rep. Monogr.* **7** 585

[2] Apollinari G *et al* 2015 *High-Luminosity Large Hadron Collider (HL-LHC): Preliminary Design Report (CERN Yellow Reports: Monographs)* CERN-2015-005, FERMILAB-DESIGN-2015-02 CERN (https://doi.org/10.5170/CERN-2015-005)

[3] Apollinari G *et al* 2015 High luminosity Large Hadron Collider HL-LHC *CERN Yellow Report* FERMILAB-DESIGN-2017-02 CERN p 1–19

[4] Baltz A J *et al* 2008 The physics of ultraperipheral collisions at the LHC *Phys. Rep.* **458** 1

[5] Jowett J M and Carli C 2006 The LHC as a proton-nucleus collider *Proc. European Particle Accelerator Conf. 2006 (Edinburgh, Scotland)* p 550 EPAC-2006-MOPLS009, (http://accelconf.web.cern.ch/AccelConf/e06/PAPERS/MOPLS009.PDF)

[6] Salgado C A *et al* 2012 Proton-nucleus collisions at the LHC: scientific opportunities and requirements *J. Phys. G: Nucl. Part. Phys.* **39** 015010

[7] Coupard J *et al* 2016 *LHC Injectors Upgrade, Technical Design Report, vol II: Ions* CERN-ACC-2016-0041 (https://cds.cern.ch/record/2153863)

[8] Klein S R 2001 Localized beam pipe heating due to e$^-$ capture and nuclear excitation in heavy ion colliders *Nucl. Instrum. Methods Phys. Res.* A **459** 51

[9] Jowett J M *et al* 2004 Limits to the performance of the LHC with ion beams *9th European Particle Accelerator Conf. (EPAC 2004) (Lucerne, Switzerland, 5–9, July 2004)*

[10] Bruce R *et al* 2007 First observations of beam losses due to bound-free pair production in a heavy-ion collider *Phys. Rev. Lett.* **99** 144801

[11] Bruce R *et al* 2009 Beam losses from ultra-peripheral nuclear collisions between (Pb-208)82+ ions in the Large Hadron Collider and their alleviation *Phys. Rev. Accel. Beams* **12** 071002

[12] Schaumann M 2015 Heavy-ion performance of the LHC and future colliders *CERN-THESIS-2015-195* Aachen, Germany: RWTH Aachen U. urn:nbn:de:hbz:82-rwth-2015-050284

[13] Braun H-H *et al* 2004 Collimation of heavy ion beams in LHC *9th European Particle Accelerator Conf. (EPAC 2004* July 5–9, 2004*) (Lucerne, Switzerland)*

[14] Hermes P *et al* 2016 Heavy-ion collimation at the Large Hadron Collider: simulations and measurements *CERN-THESIS-2016-230* (https://cds.cern.ch/record/2241364)

[15] Hermes P *et al* 2016 Measured and simulated heavy-ion beam loss patterns at the CERN Large Hadron Collider *Nucl. Instrum. Methods Phys. Res.* A **819** 73

[16] Jowett J *et al* 2016 Bound-free pair production in LHC Pb–Pb operation at 6.37 Z TeV per beam *Proc. Int. Particle Accelerator Conf. 2016 (Busan, Korea)* p 1497 IPAC-2016- TUPMW028

[17] Castro C B *et al* 2016 Power deposition in LHC magnets due to bound-free pair production in the experimental insertions *Proc. Int. Particle Accelerator Conf. 2016 (Busan, Korea)* p 1418 IPAC-2016-TUPMW006

[18] Hermes P *et al* 2015 Betatron cleaning for heavy ion beams with IR7 dispersion suppressor collimators *Proc. Int. Particle Accelerator Conf. 2016 (Richmond, USA)* p 2057 IPAC-2015-TUPTY025, (http://accelconf.web.cern.ch/AccelConf/IPAC2015/papers/tupty025.pdf)

[19] Apollinari G *et al* 2017 *High-Luminosity Large Hadron Collider (HL-LHC) (CERN Yellow Reports: Monographs Vol. 7)* CERN-2017-007-M CERN (https://doi.org/10.23731/CYRM-2017-004)

[20] Citron Z *et al* 2018 Future physics opportunities for high-density QCD at the LHC with heavy-ion and proton beams *(CERN Yellow Reports: Monographs Vol. 7)* CERN-LPCC-2018-07 CERN arXiv:1812.06772 [hep-ph]

[21] Jowett J 2018 HL-LHC performance: update for HE-LHC and light ions *Workshop on the physics of HL-LHC, and perspectives at HE-LHC (CERN. Geneva, Switzerland)* (https://indico.cern.ch/event/686494/timetable)

[22] Schaumann M *et al* 2018 First xenon–xenon collisions in the LHC *Proc. 9th Int. Particle Accelerator Conf. (IPAC 2018) (Vancouver, BC, Canada, 29 April–4 May, 2018)* MOPMF039 (https://doi.org/10.18429/JACoW-IPAC2018-MOPMF039)

[23] Budnev V M *et al* 1975 The two photon particle production mechanism. Physical problems. Applications. Equivalent photon approximation *Phys. Rep.* **15** 181

[24] Harland-Lang L A, Khoze V A and Ryskin M G 2019 Exclusive LHC physics with heavy ions: SuperChic 3 *Eur. Phys. J.* C **79** 39

[25] Knapen S *et al* 2017 Searching for axionlike particles with ultraperipheral heavy-ion collisions *Phys. Rev. Lett.* **118** 171801

[26] CMS 2018 Evidence for light-by-light scattering and searches for axion-like particles in ultraperipheral PbPb collisions at $\sqrt{S_{NN}} = 5.02$ TeV *Phys. Lett.* B **797** 134826

[27] LHC Forward Physics 2016 LHC forward physics *J. Phys. G: Nucl. Part. Phys.* **43** 110201

[28] ATLAS 2015 *Technical Design Report for the ATLAS Forward Proton Detector* CERNLHCC-2015-009, ATLAS-TDR-024

[29] CMS, TOTEM 2014 *CMS-TOTEM Precision Proton Spectrometer* CERN-LHCC-2014- 021, TOTEM-TDR-003, CMS-TDR-13

[30] FP420 R&D 2009 The FP420 R&D project: Higgs and new physics with forward protons at the LHC *J. Instrum.* **4** T10001

[31] Klein S R *et al* 2017 STARlight: a Monte Carlo simulation program for ultra-peripheral collisions of relativistic ions *Comput. Phys. Commun.* **212** 258

[32] d'Enterria D and Lansberg J-P 2010 Study of Higgs boson production and its b anti-b decay in gamma-gamma processes in proton-nucleus collisions at the LHC *Phys. Rev.* D **81** 014004

[33] Peccei R D and Quinn H R 1977 CP conservation in the presence of instantons *Phys. Rev. Lett.* **38** 1440

[34] Wilczek F 1978 Problem of strong P and T invariance in the presence of instantons *Phys. Rev. Lett.* **40** 279

[35] d'Enterria D and da Silveira G G 2013 Observing light-by-light scattering at the Large Hadron Collider *Phys. Rev. Lett.* **111** 080405
     d'Enterria D and da Silveira G G 2016 Observing light-by-light scattering at the Large Hadron Collider *Phys. Rev. Lett.* **116** 129901 (erratum)

[36] ATLAS 2017 Evidence for light-by-light scattering in heavy-ion collisions with the ATLAS detector at the LHC *Nat. Phys.* **13** 852

[37] ATLAS 2019 Observation of light-by-light scattering in ultraperipheral Pb+Pb collisions with the ATLAS detector *Phys. Rev. Lett.* **123** 052001

[38] Knapen S *et al* 2017 LHC limits on axion-like particles from heavy-ion collisions arXiv:1709.07110 [hep-ph]

[39] Dolan M J *et al* 2017 Revised constraints and Belle II sensitivity for visible and invisible axionlike particles *J. High Energy Phys.* JHEP12(2017)094

[40] Born M and Infeld L 1934 Foundations of the new field theory *Proc. R. Soc.* A **144** 425

[41] Fradkin E S and Tseytlin A A 1985 Nonlinear electrodynamics from quantized strings *Phys. Lett.* B **163** 123

[42] Ellis J, Mavromatos N E and You T 2017 Light-by-light scattering constraint on Born–Infeld theory *Phys. Rev. Lett.* **118** 261802

[43] Gomis J *et al* 2000 Noncommutative gauge dynamics from the string world sheet *J. High Energy Phys.* JHEP08(2000)011

[44] Hewett J L, Petriello F J and Rizzo T G 2001 Signals for noncommutative interactions at linear colliders *Phys. Rev.* D **64** 075012

[45] Richard F 2017 Search for a light radion at HL-LHC and ILC250 arXiv:1712.06410 [hep-ex].

[46] Cheung K-M 2000 Diphoton signals for low scale gravity in extra dimensions *Phys. Rev.* **D61** 015005

[47] Davoudiasl H 1999 $\gamma\gamma \to \gamma\gamma$ as a test of weak scale quantum gravity at the NLC *Phys. Rev.* D **60** 084022

[48] Cakir O and Ozansoy K O 2008 Unparticle searches through $\gamma\gamma$ scattering *Eur. Phys. J.* C **56** 279

[49] Grinstein B, Intriligator K A and Rothstein I Z 2008 Comments on unparticles *Phys. Lett.* B **662** 367

[50] Delgado A and Strassler M J 2010 A simple-minded unitarity constraint and an application to unparticles *Phys. Rev.* D **81** 056003

[51] Kathrein S, Knapen S and Strassler M J 2011 Bounds from LEP on unparticle interactions with electroweak bosons *Phys. Rev.* D **84** 015010

[52] Beresford L and Liu J 2018 Photon collider search strategy for sleptons and dark matter at the LHC *Phys. Rev. Lett.* **123** 141801

[53] Harland-Lang L A *et al* 2019 LHC searches for dark matter in compressed mass scenarios: challenges in the forward proton mode *J. High Energy Phys.* JHEP04(2019)010
[54] Dirac P A M 1931 Quantised singularities in the electromagnetic field *Proc. R. Soc.* A **133** 60
[55] Kurochkin Y *et al* 2006 On production of magnetic monopoles via $\gamma\gamma$ fusion at high energy pp collisions *Mod. Phys. Lett.* A **21** 2873
[56] Epele L N *et al* 2012 Looking for magnetic monopoles at LHC with diphoton events *Eur. Phys. J. Plus* **127** 60
[57] Reis J T and Sauter W K 2017 Production of magnetic monopoles and monopolium in peripheral collisions *Phys. Rev.* D **96** 075031
[58] Baines S *et al* 2018 Monopole production via photon fusion and Drell–Yan processes: MadGraph implementation and perturbativity via velocity-dependent coupling and magnetic moment as novel features *Eur. Phys. J.* C **78** 966
[59] Fanchiotti H, Garcia Canal C A and Vento V 2017 Multiphoton annihilation of monopolium *Int. J. Mod. Phys.* **A32** 1750202
[60] Ginzburg I F and Panfil S L 1982 The possibility of observation of heavy Dirac–Schwinger magnetic pole *Sov. J. Nucl. Phys.* **36** 850
Ginzburg I F and Panfil S L 1982 The possibility of observation of heavy Dirac–Schwinger magnetic pole *Yad. Fiz.* **36** 1461
[61] Ginzburg I F and Schiller A 1998 Search for a heavy magnetic monopole at the Tevatron and CERN LHC *Phys. Rev.* D **57** 6599
[62] D0 1998 A search for heavy pointlike Dirac monopoles *Phys. Rev. Lett.* **81** 524
[63] Gamberg L P, Kalbfleisch G R and Milton K A 2000 Direct and indirect searches for low mass magnetic monopoles *Found. Phys.* **30** 543
[64] Milton K A 2006 Theoretical and experimental status of magnetic monopoles *Rep. Prog. Phys.* **69** 1637
[65] Preskill J 1984 Magnetic monopoles *Annu. Rev. Nucl. Part. Sci.* **34** 461
[66] Polchinski J 2004 Monopoles, duality, and string theory *Int. J. Mod. Phys.* A **19S1** 145
[67] Particle Data Group 2018 Review of particle physics *Phys. Rev.* D **98** 030001
[68] MoEDAL 2018 Search for magnetic monopoles with the MoEDAL forward trapping detector in 2.11 fb^{-1} of 13 TeV proton–proton collisions at the LHC *Phys. Lett.* B **782** 510
[69] 't Hooft G 1974 Magnetic monopoles in unified gauge theories *Nucl. Phys.* B **79** 276
[70] Polyakov A M 1974 Particle spectrum in the quantum field theory *JETP Lett.* **20** 194
[71] Witten E 1979 Baryons in the $1/N$ expansion *Nucl. Phys.* B **160** 57
[72] Drukier A K and Nussinov S 1982 Monopole pair creation in energetic collisions: is it possible? *Phys. Rev. Lett.* **49** 102
[73] Papageorgakis C and Royston A B 2014 Revisiting soliton contributions to perturbative amplitudes *J. High Energy Phys.* JHEP09(2014)128
[74] Goebel C J 1970 *The Spatial Extent of Magnetic Monopoles* (Chicago, IL: University of Chicago Press) p 338
[75] Huang X-G 2016 Electromagnetic fields and anomalous transports in heavy-ion collisions. A pedagogical review *Rep. Prog. Phys.* **79** 076302
[76] Affleck I K and Manton N S 1982 Monopole pair production in a magnetic field *Nucl. Phys.* B **194** 38
[77] He Y D 1997 Search for a Dirac magnetic monopole in high-energy nucleus–nucleus collisions *Phys. Rev. Lett.* **79** 3134
[78] Gould O and Rajantie A 2017 Magnetic monopole mass bounds from heavy ion collisions and neutron stars *Phys. Rev. Lett.* **119** 241601
[79] Drewes M *et al* 2020 Searching for new long lived particles in heavy ion collisions at the LHC *Phys. Rev. Lett.* **124** 081801
[80] Curtin D *et al* 2019 Long-lived particles at the energy frontier: the MATHUSLA physics casear *Rept. Prog. Phys.* **82** 116201
[81] Alimena J *et al* 2019 Searching for long-lived particles beyond the standard model at the Large Hadron Collider arXiv:1903.04497 [hep-ph]
[82] Drewes M *et al* 2020 New long-lived particle searches in heavy-ion collisions at the LHC *Phys. Rev.* D **101** 055002
[83] CMS 2017 Observation of top quark production in proton-nucleus collisions *Phys. Rev. Lett.* **119** 242001

[84] Asaka T and Shaposhnikov M 2005 The ν MSM, dark matter and baryon asymmetry of the Universe *Phys. Lett.* B **620** 17

[85] PHENIX 2015 Search for dark photons from neutral meson decays in $p + p$ and $d + $ Au collisions at $\sqrt{s_{NN}} = 200$ GeV *Phys. Rev.* C **91** 031901

[86] Ilten P *et al* 2016 Proposed inclusive dark photon search at LHCb *Phys. Rev. Lett.* **116** 251803

[87] Pierre Auger 2015 Muons in air showers at the Pierre Auger observatory: mean number in highly inclined events *Phys. Rev.* D **91** 032003
      Pierre Auger 2015 Muons in air showers at the Pierre Auger observatory: mean number in highly inclined events *Phys. Rev.* **91** 059901 (erratum)

[88] Baur S *et al* 2019 The ratio of electromagnetic to hadronic energy in high energy hadron collisions as a probe for collective effects, and implications for the muon production in cosmic ray air showers arXiv:1902.09265 [hep-ph]

[89] Farrar G R 2017 Stable sexaquark arXiv:1708.08951 [hep-ph]

[90] Jaffe R L 1977 Perhaps a stable dihyperon *Phys. Rev. Lett.* **38** 195
      Jaffe R L 1977 Perhaps a stable dihyperon *Phys. Rev. Lett.* **38** 617 (erratum)

[91] Farrar G R 2018 A precision test of the nature of dark matter and a probe of the QCD phase transition arXiv:1805.03723 [hep-ph]

[92] Gross C *et al* 2018 Dark matter in the standard model? *Phys. Rev.* D **98** 063005

[93] McDermott S D, Reddy S and Sen S 2019 Deeply bound dibaryon is incompatible with neutron stars and supernovae *Phys. Rev.* D **99** 035013

[94] Kolb E W and Turner M S 2019 Dibaryons cannot be the dark matter *Phys. Rev.* D **99** 063519

[95] Witten E 1984 Cosmic separation of phases *Phys. Rev.* **D30** 272

[96] Abhishek A and Mishra H 2019 Chiral symmetry breaking, color superconductivity, and the equation of state for magnetized strange quark matter *Phys. Rev.* D **99** 054016

[97] Kharzeev D E, McLerran L D and Warringa H J 2008 The effects of topological charge change in heavy ion collisions: event-by-event P and CP violation *Nucl. Phys.* A **803** 227

[98] AMS 2015 Precision measurement of the proton flux in primary cosmic rays from rigidity 1 GV to 1.8 TV with the alpha magnetic spectrometer on the international space station *Phys. Rev. Lett.* **114** 171103

[99] Genolini Y *et al* 2018 Current status and desired precision of the isotopic production cross sections relevant to astrophysics of cosmic rays: Li, Be, B, C, and N *Phys. Rev.* C **98** 034611

[100] Donato F, Korsmeier M and Di Mauro M 2017 Prescriptions on antiproton cross section data for precise theoretical antiproton flux predictions *Phys. Rev.* D **96** 043007

[101] AMS 2016 Antiproton flux, antiproton-to-proton flux ratio, and properties of elementary particle fluxes in primary cosmic rays measured with the alpha magnetic spectrometer on the international space station *Phys. Rev. Lett.* **117** 091103

[102] Cuoco A, Kraemer M and Korsmeier M 2017 Novel dark matter constraints from antiprotons in light of AMS-02 *Phys. Rev. Lett.* **118** 191102

[103] Cui M-Y *et al* 2017 Possible dark matter annihilation signal in the AMS-02 antiproton data *Phys. Rev. Lett.* **118** 191101

[104] Cuoco A *et al* 2017 Probing dark matter annihilation in the Galaxy with antiprotons and γ rays *J. Cosmol. Astropart. Phys.* JCAP10(2017)053

[105] Cui M-Y *et al* 2018 Revisit of cosmic ray antiprotons from dark matter annihilation with updated constraints on the background model from AMS-02 and collider data *J. Cosmol. Astropart. Phys.* JCAP06(2018)024

[106] Reinert A and Winkler M W 2018 A precision search for WIMPs with charged cosmic rays *J. Cosmol. Astropart. Phys.* JCAP01(2018)055

[107] LHCb 2018 Measurement of antiproton production in p-He collisions at $\sqrt{s_{NN}} = 110$ GeV *Phys. Rev. Lett.* **121** 222001

[108] Korsmeier M, Donato F and Di Mauro M 2018 Production cross sections of cosmic antiprotons in the light of new data from the NA61 and LHCb experiments *Phys. Rev.* D **97** 103019

[109] Cuoco A *et al* 2019 Scrutinizing the evidence for dark matter in cosmic-ray antiprotons *Phys. Rev.* D **99** 103014

[110] ALICE 2018 Production of deuterons, tritons, ^{3}He nuclei and their antinuclei in pp collisions at $\sqrt{s} = 0.9, 2.76$ and 7 TeV *Phys. Rev.* C **97** 024615

[111] d'Enterria D *et al* 2011 Constraints from the first LHC data on hadronic event generators for ultra-high energy cosmic-ray physics *Astropart. Phys.* **35** 98

[112] HiRes M I A 2000 Evidence for changing of cosmic ray composition between 1017-eV and 1018-eV from multicomponent measurements *Phys. Rev. Lett.* **84** 4276

[113] Pierre Auger 2016 Testing hadronic interactions at ultrahigh energies with air showers measured by the Pierre Auger observatory *Phys. Rev. Lett.* **117** 192001

[114] EAS-MSU IceCube KASCADE-Grande NEVOD-DECOR Pierre Auger SUGAR Telescope Array Yakutsk EAS Array 2019 Report on tests and measurements of hadronic interaction properties with air showers *EPJ Web Conf.* **210** 02004

[115] d'Enterria D, Pierog T and Sun G 2019 Impact of QCD jets and heavy-quark production in cosmicray proton atmospheric showers up to 1020 eV *Astrophys. J.* **874** 152

[116] Brooijmans G, Schichtel P and Spannowsky M 2016 Cosmic ray air showers from sphalerons *Phys. Lett.* B **761** 213